ELSEVIER

Nuclear Instruments and Methods in Physics Research A 459 (2001) 247–255

NUCLEAR INSTRUMENTS & METHODS IN PHYSICS RESEARCH Section A

www.elsevier.nl/locate/nima

A neutron detector for cold fusion experiments

E. Cisbani[a], G.M. Urciuoli[a,*], S. Frullani[a], F. Garibaldi[a], F. Giuliani[a], D. Gozzi[b], M. Gricia[a], M. Iodice[a], M. Lucentini[a], F. Santavenere[a]

[a]*Physics Laboratory, Istituto Superiore di Sanità and Instituto Nazionale di Fisica Nucleare Roma, gruppo collegato Sanità, viale Regina Elena 299, I-00161 Rome, Italy*

[b]*Dipartimento di Chimica, Università di Roma "La Sapienza", piazzale Aldo Moro 1, I-00185 Rome, Italy*

Received 6 April 2000; received in revised form 10 August 2000; accepted 10 August 2000

Abstract

This paper describes a neutron detector designed by INFN-Sanità group of Rome. The detector fulfills all the requirements of cold fusion experiments and, on the other hand, can operate in several kind of experiments involving neutron detection, even when significant, variable and not taggable background is present. As a matter of fact, it is suitable to detect every source emitting multi-MeV neutrons, correlated or not correlated, in burst or constant rate, isotropic or directional. It is a low-noise detector. The detector was used in cold fusion experiments demonstrating, with high sensibility, the absence of neutron emission in these phenomena.

PACS: 29.40

Keywords: Neutron; Neutron detectors; Cold fusion; Background analysis

1. Introduction

The need of a high efficiency, large angular acceptance, low noise, reliable neutron detector is a strong issue in cold fusion experiments. In fact, the background subtraction is a very hard matter due to the fluctuation of the background itself and the lack of a trigger that tags neutrons. In addition, standard neutron detectors are very sensible to electromagnetic noise. One important issue on cold fusion experiments is also the detection of possible source of correlated neutrons (both in space and in time). At last, to improve the very poor efficiency of standard neutron counters, a large angular acceptance detector is needed. To achieve all these performances, the INFN-Sanità group of Rome has developed a unique, toroidal shape, large angular acceptance, segmented and rotating around its axis neutron detector with a data acquisition system oriented to the detection of correlated signals.

This paper describes the design of the detector which has been used in several Fleishmann–Pons like experiments in a collaboration between INFN Sanità and Dipartimento di Chimica of the "La Sapienza" University in Rome. The geometry and constituting elements of the detector are described in Section 2. The details of the data acquisition system, the detector efficiency and the results obtained in the experiments are illustrated in Sections 3–5, respectively.

* Corresponding author. Tel.: +39-0644-57165; fax: +39-0649-387075.

E-mail address: urciuoli@axiss.iss.infn.it (G.M. Urciuoli).

0168-9002/01/$ - see front matter
PII: S0168-9002(00)01003-2

2. Geometry and elements

The detector has been manufactured by Jomar System Division of Canberra Industries Inc. according to the specifications and on the basis of a preliminary design of the INFN-Sanità group of Rome. The detector geometry is shown in Figs. 1 (top view) and 2 (cross-section). The active part of the detector has a toroidal, 687 mm high, shape; its outer and the inner diameters are 711 and 508 mm, respectively.

The toroid is essentially a neutron moderator made up of polyethylene surrounded by aluminum and steel. A 290 mm diameter plug in the bottom part of the moderator is removable for ease of operation. In the moderator are inserted two rings of 30 neutron counters each, consisting of ^{3}He-filled proportional counters (cylinders with an anodic wire along their axis). The counters detect the thermalized neutron by means of the reaction $^3\mathrm{He} + \mathrm{n} \rightarrow {}^3\mathrm{H} + \mathrm{p} + 0.765\ \mathrm{MeV}$, collecting on their anodic wire the electrons generated by the triton and proton tracks in the helium by ionization of the gas.

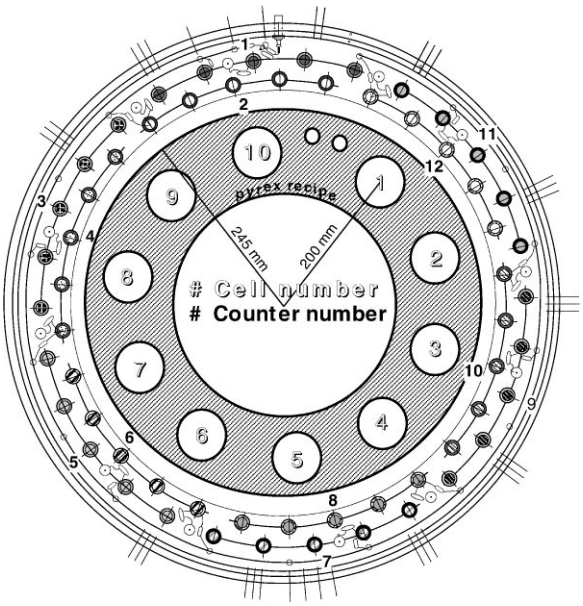

Fig. 1. The top view of the detector (outer ring) surrounding the pyrex vessel with the 10 electrolytic cells, as in the cold fusion experimental set-up.

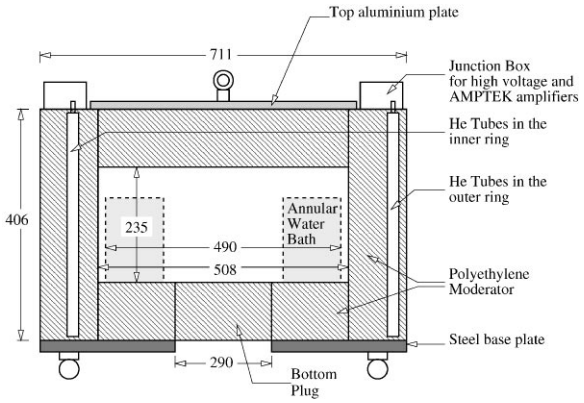

Fig. 2. The cross-view of the detector with the annular water vessel used in the cold fusion experiments. Units are mm.

Each counter is a stainless-steel tube, whose diameter is 25.4 mm and whose effective length is 406 mm (there is an additional of 25.4 mm at the bottom and 50.8 mm at the top for connectors). The ^{3}He pressure in the tubes is 6 atm.

The counters are assembled in order to form 12 groups. These groups are placed along two circles (six for each circle). The counters of the outer ring are staggered with respect to the counters of the inner one (see Fig. 1). The 12 groups of neutron counters can be considered as independent detectors by themselves and in the following they will be referred to as "subdetectors".

The five counters of each group are wired to a circuit board in the junction box (see Fig. 2) which distributes the high voltage to the counters and provides a common preamplification and discrimination stages to the counters signals; both analog and digital outputs from these stages are processed by the data acquisition electronics (Section 3). The detector can rotate around its axis.

In cold fusion experiments, a toroidal Pyrex vessel of water, embedding the electrochemical cells, was housed in the room inside the detector in order to measure the heat excess. The water vessel has an outer diameter of 490 mm. The distance between the axis of the detector and the axis of each cell is 200 mm (Fig. 1). As many as 10 different cells were placed in the vessel. The geometrical solid angle covered by the whole detector with respect to a source placed at its center is 7.89 sr while the

geometrical solid angle covered by the whole detector with respect to an electrolytic cell is 12.15 sr (taking into account only the sensitive part of the ^{3}He tubes).

The toroidal shape and segmentation of the detector make it easy to localize a neutron source placed in it and cuts down the cumbersome problem of the subtraction of the background that arises in cold fusion experiments because of the lack of trigger. As a matter of fact, background neutrons are expected to fire the subdetectors in the outer layer more often than those in the inner one. Moreover, an increase of background is expected to enhance the counting rates of all the subdetectors in a proportional way. On the other hand, if an electrolytic cell inside the detector emits neutrons, the counting rate of the subdetectors near to it will increase with respect to the others and the subdetector placed in the inner ring will count more than those in the outer one. At last, counting rate enhancements of one or more subdetectors due to misfunctionings are easily discovered by rotating the whole detector around its axis and placing this way new subdetectors near the hypothetical source of neutrons. An additional control on misfunctionings performed by wave shape analysis of the electronic pulses from the subdetectors is described in the Section 3.

3. The data acquisition and analysis system

The data acquisition system was designed to disentangle a neutron source from the environmental poissonian neutron background, which was of the order of $m_b = 4$ counts/min per subdetector. In this context, a neutron source appears as a deviation from the poissonian distribution of the background. Such deviation has been checked in different ways:

- neutron counting rate (measured at 3 time scales) off at least 3 sigma from the background average. As a matter of fact, a counts enhancement of 3 standard deviations of the background in the interval ΔT ($3\sqrt{m_b \Delta T}$) is a tag for a high probable presence of a neutron source. Three multichannel devices were used for this purpose, with each subdetector connected to one channel of one device: one Camac scalar recorded at the end of a run ('long' time interval lasting several hours), one Camac scalar read and cleared at fixed frequency ('short', typically 10 min, interval), and a Pattern Unit that recorded a signal occurrence both in time and in subdetector number ('very short' time interval); the Pattern Unit time resolution (due to the data acquisition dead time) was 1 ms.

  A neutron source emitting 20 neutrons in few seconds, due to efficiency (see Section 4), would have caused only 2 counts in a subdetector. This amount, well above the background in interval shorter than a minute, is negligible in longer period of time; for this reason different time scales have been investigated.
- Events distributions in 'short' intervals not fitted by a poissonian curve with $\mu = m_b \Delta T$. In this case, the χ^2 test gives the confidence level of the fit and then the rejection of a source hypothesis.
- Events time interval distribution off the poissonian statistics. The distribution of the time intervals between two consecutive detected neutrons was histogrammed by a TDC connected to a histogramming memory (a LeCroy 3588 module). The histogram was checked and cleared after each run.

Fluctuations of the background have been taken into account evaluating m_b for each analysis and looking at spatial correlation between neutrons up to the ms time scale. The neutron sources can be localized by checking simultaneous increases of counting rates: when a neutron source is placed in one cell, the counting rate of each subdetectors close to it as well as the rates of the coincidences between these subdetectors shall increase. A count enhancement in one subdetector only is likely to be due to misfunctionings. The Camac Pattern Unit was used for this purpose, the coincidence-time interval between two subdetectors was of about 1 ms.

Moreover, the possibility of strongly time-correlated neutrons (below the μs scale) has been considered employing a dedicated Neutron Coincidence Analyzer, the Jomar Shift-Register (JSR)

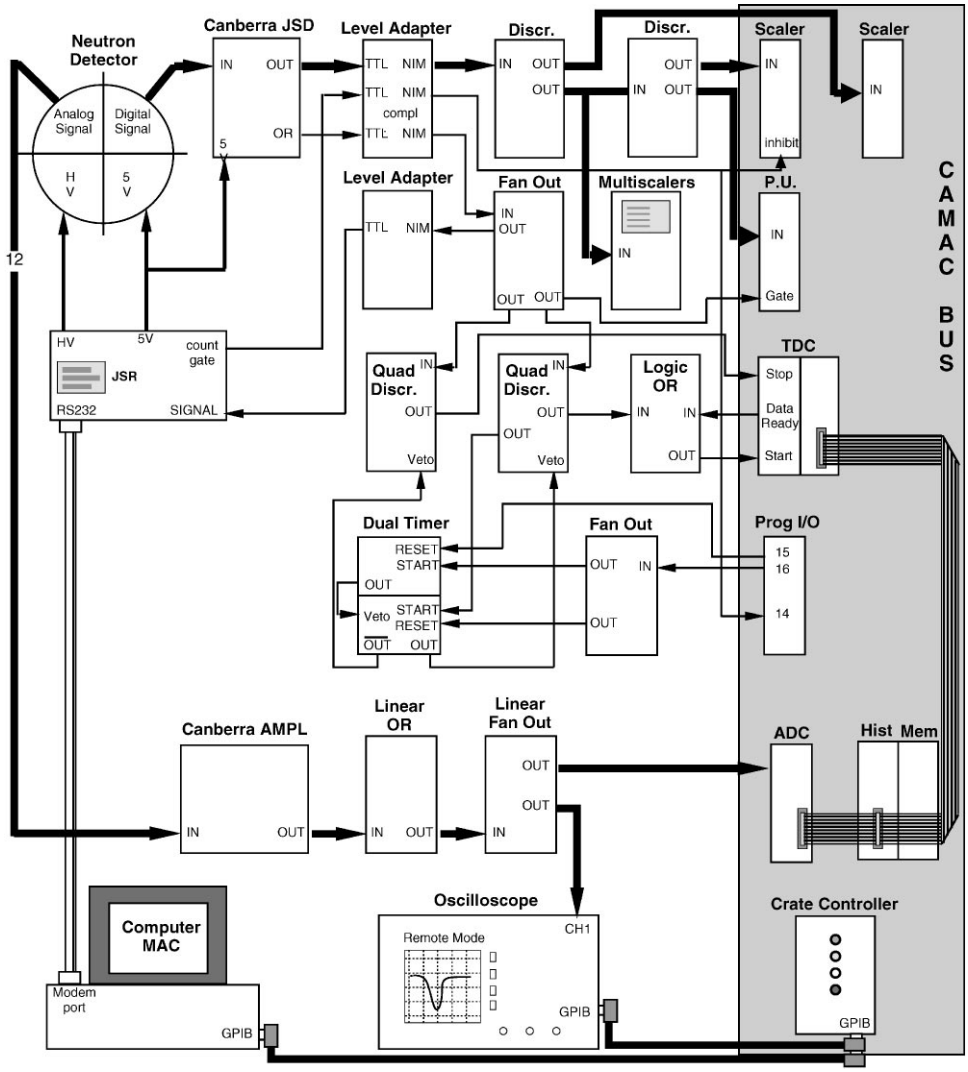

Fig. 3. The data acquisition system. Thick lines stand for groups of 12 signals, while thin ones stand for single signals. Refer to Table 1 for the list of modules.

which is described below (see Section 3.1). The presence of 'extremely short time' (μs scale) correlated neutron emissions hence could have been a tag for cold fusion events in the hypothesis that this kind of phenomena have a burst structure.

Finally, the acquisition system includes a redundant check of sparks and/or electronics misfunctioning through the acquisition of the shape and integral charge value of the analog pulses. Two devices were used for these purposes: one LeCroy 3512 buffered ADC connected to a histogramming memory and one buffered oscillosope. Both tools acquired the pulses coming from the analog OR of the 12 subdetectors (Fig. 3). The integral charge of the pulses were digitized by the ADC (Table 1). The ^{3}He filled proportional counters detect only termalized neutron (in our case neutrons were termalized by the polyethylene moderator) and their spectra have the typical shape shown in Fig. 4, with an artificial cut at low energy due to the trigger

Table 1
Detailed list of the electronics modules and equipments used in the data acquisition

NIM modules	
Level adapter	LeCroy LRS 688AL. Compl. TTL/NIM
Fan out	CAEN N105
Discr.	CAEN N96
Linear OR, Logic OR	CAEN N113
Quad discr.	LeCroy 821. Mode: Update only
Linear fan out	LeCroy 428F. Mode: Normal
Dual timer	CAEN N2255B. Delay = ∞
Multiscalar	Borel multiscalar. Output on the monitor
Canberra AMPL	Canberra ND247 AMP (dedicated)
Fan out	CAEN N401
CAMAC modules	
P.U.	SEN 16P2047. Rear panel GL
Prog. I/O	CAEN C219
Scalar	LeCroy 2551
ADC	LeCroy 3521. Mode PD, Polarity + ,AntiCOIN
Hist mem	LeCroy 3588
Crate controller	LeCroy 8901A
Other equipments	
Oscilloscope	LeCroy 9310L
Computer	Macintosh IIFX, 32 Mbyte RAM, 0.5 Gbyte HD
External storage	PLI infinity 40 Turbo
GPIB – NuBus interface	National instruments NB-6PIB

threshold. Deviations of our ADC spectra from the standard one were hence a control on electronic misfunctionings.

The oscilloscope acquired the shape of the single signal and the time of its occurrence. When an enhancement of the neutron count rate was detected, one could check the shape of the signal(s) in question. Single-noise signals with many oscillations around zero could, in fact, generate "false" count enhancements. Fig. 5a shows two standard regular pulses (intentionally overlapped) by true events. Fig. 5b shows two pulses registered by the oscilloscope when electromagnetic noise was induced on a ^{3}He counter. The pulses are intentionally overlapped to a good one. The oscilloscope provided a powerful check of sparks that caused big enhancement of both JSR and scale counts (see below).

To keep track of the experimental trend one Borel multiscalar with output on a monitor was used to detect "on-line" counting rate enhancements of some subdetectors. In this way, additional checks on the detector could be performed. If, for instance, a subdetector counting rate increased, a manual rotation of the whole detector round its axis would be performed. If, after this operation, the counting rate of the subdetector in question (facing now other cells) was still high, an electronic misfunctioning was surely the cause of its behaviour. Note that the presence of a source inside of a cell enhances the counting rate only in the surrounding subdetectors and makes the rate of the inner ring subdetectors higher than the rate of the outer ring ones. General increasing of the rates of all subdetectors, especially when the external ring ones are higher, are very probably due to an increase of the neutron background.

The data acquisition system is schematically shown in Fig. 3. One Macintosh IIFX computer drives the CAMAC modules and one LeCroy 9310L oscilloscope through a GPIB interface and the JSR by a RS232 line.

The 12 analog signals coming from the subdetectors were amplified, linearized and finally delivered to the digital oscilloscope and to the LeCroy 3512 buffered ADC. The ADC transferred its digitized values to the LeCroy 3588 CAMAC histogramming memory that is read and displayed on the computer at a fixed frequency.

The digital oscilloscope reads and stores in its memory buffer shape of single signals and the time of their occurrence. Each time the oscilloscope buffer became 95% full, an interrupt was sent through the GPIB interface to the Macintosh which collected the data from the buffer to its RAM memory and then to the storage system; the buffer was then cleared. Typical figures were: 100 points per pulse and 1000 waveforms in the oscilloscope memory.

The 12 digital pulses from the subdetectors were converted into TTL signals by the Jomar System Discriminator (JSD) module, which provided 12 independent TTL signals and a single OR of the 12 lines. Each of the 12 individual TTL signals were converted to NIM and fanned out to three scalars and one pattern unit.

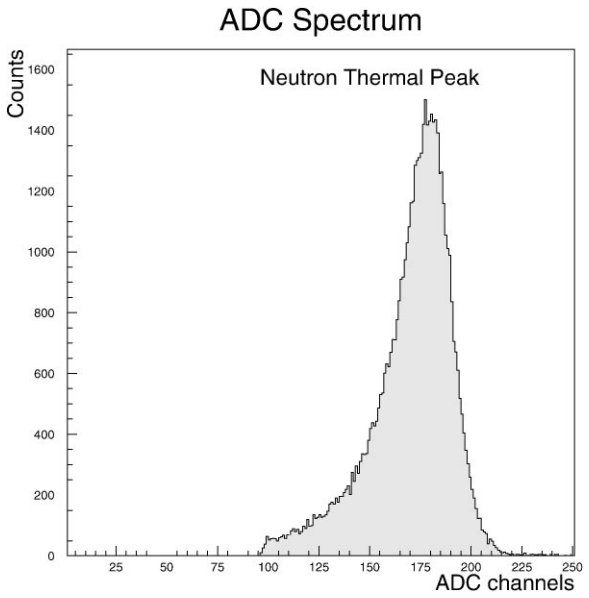

Fig. 4. The typical ADC spectrum of one subdetector. The peak (called the thermal peak) corresponds to the case in which all the Q of the reaction $^3He + n \rightarrow {}^3H + p + 0.765$ MeV is deposited in the counter gas.

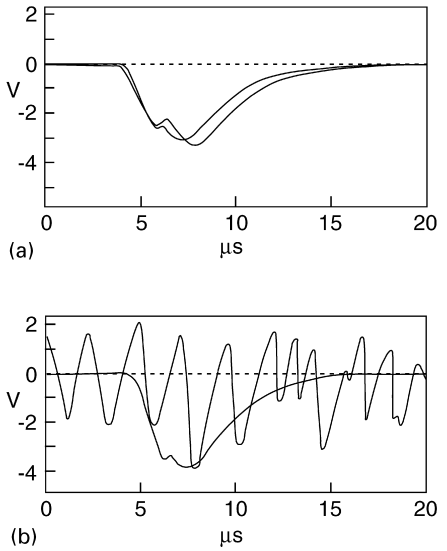

Fig. 5. Top plot: two typical good signals at the digital oscilloscope, overimposed for comparison. Bottom plot: an uncommon noise pulse compared with a good signal.

A 12 channel scalar was read and cleared at fixed time ("short time" scalar). Another scalar cleared at the beginning of the run and read at the end giving the total events on each subdetectors ("long time" scalar). A third scalar was connected to a monitor display, allowing visual checking of neutron count enhancements.

The Pattern Unit detected coincidences (within one ms) between signals from subdetectors. In the meantime, the OR of the previous signals were sent to one LeCroy 4204 TDC module and to the JSR-12 dedicated module.

The TDC was used for the detection of time intervals between adjacent signals (the CAMAC histogramming memory produced the distribution of the time intervals). The TDC operated in single Start–multiple STOP mode: when a given burst of signals came out from the neutron detector, the relative pulses were sent to two discriminators working as veto modules. As shown in Fig. 3, one discriminator was connected to the START of the TDC and to a dual timer, the other one to the TDC STOP and to a second dual timer. The dual timers provided veto signals in such a way that only the first pulse of the given burst produced the TDC START, while all the others gave the STOP.

After each time to digit conversion, a DATA READY signal was sent by the TDC to its START input to restart time interval measurements again. The TDC gave the distribution of the time intervals between events in a run (time resolution 500 ns) and it was hence a tool for detecting neutron emission correlation.

Some of the modules described above accept only NIM pulses. As a consequence the data acquisition system used several TTL-NIM adapters (see Fig. 3).

3.1. The dedicated JSR-12

This is quite a sophisticated module [1], designed by Jomar System Division, that was able to distinguish between coincidence neutron events emitted in few microseconds and background. The basic idea lays on the fact that the number of events in a burst of correlated neutrons decreases sharply with the time. The events registered in a time window opened much later than the beginning of the

burst, should count hence just background events (accidental coincidences). As a consequence, if we suppose that neutrons in bursts are emitted essentially in few tens of microseconds, we can measure the number of "real" coincidences in a burst just opening two-time windows, one during the burst itself and the other one millisecond later or so, and subtracting the neutron counts registered in them.

The JSR-12 has three counter registers: T (total events), $R + A$ (real and accidental) and A (accidental). For each neutron detected the JSR-12 increments the T register by 1 and opens two gates (windows): prompt (4.5 μs later) and delayed (1.024 ms later) gates whose widths are programmable from 1 to 250 μs. All events occurring in the prompt (delayed) gate are considered "simultaneous" and counted in the $R + A$ (A) register.

Opening one window for each neutron avoids long dead time (in this way, the system does not wait for the expire of the second time window), but makes it possible for a neutron to be counted more than one time in both scalars, because its occurrence can happen in more than one window (as an example, Fig. 6 shows a distribution where 9 pulses results in a value of accumulated coincidence counts equal to 12). In the worst case, when N neutrons are detected within the time interval of a single gate, the increment of the $R + A$ counter is equal to $N(N - 1)/2$.

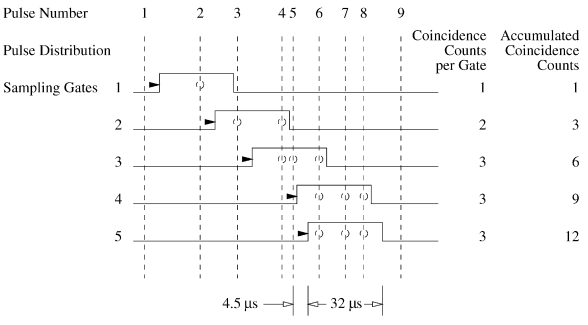

Fig. 6. An example of timing of the JSR. 4.5 μs after the detection of each pulse, a window 32 μs long is open. In the window relative to the pulse N. 1, only the pulse N. 2 is detected and the $R + A = 1$ after the first pulse. In the window relative to the pulse N. 2, the pulses N. 3 and 4 are detected. $R + A = 1 + 2 = 3$ as consequence. After the fifth pulses $R + A = 1 + 2 + 3 + 3 + 3 = 12$.

The JSR-12 input is equipped with a burst buffer, which can collect up to 16 pulses as close as 20 ns apart. The JSR-12 processes (incrementing the proper registers) these pulses with a frequency of 250 ns. Bursts of neutron signals are hence properly processed, providing that there are not more than 16 of them in the time it takes to unload the burst buffer.

JSR-12 is a powerful tool for the detection of correlated sources of neutrons. Because of its operational way, JSR-12 is not able to detect correlated emissions lasting some millisecond or more. In this case, the CAMAC scalars are suitable. The three registers of JSR-12 are read and cleared at fixed frequency (typically few minutes).

4. Efficiency

Fig. 7a shows the efficiency of the detector measured detecting the neutrons emitted by a calibration source of ^{252}Cf. This was placed at its center and at the centers of the 10 cells (used in cold fusion experiments) located in the Pyrex torus inside the detector. In the figure, *Emissions* are the neutrons predicted by the well known activity of the source, *Total* are the counts registered by the scalar read at the end of each run, and *Cumul* are the sum of the counts read and cleared at fixed 'short' time interval[1] (few minutes).

The efficiency of the detector with the source placed in one of the ten cells and at the center of the detector is 22% and 13%, respectively. The ratio between the two efficiencies equals the ratio of the effective solid angles seen by the source in the two positions (7.89 and 12.15 sr, respectively). The dependence of the efficiency on the cell position is less than 1%.

Fig. 7b and c show in detail the efficiency of each subdetector when the ^{252}Cf source was placed in cells 6 and 7 respectively. Only the four groups nearest to the source (see Fig. 1) registered significant enhancement of their counts, allowing the clean localization of the emitting cell. It should be

[1] The *Cumul*/*Total* ratio gives the inefficiency of the data acquisition system due to the dead time, which was negligible.

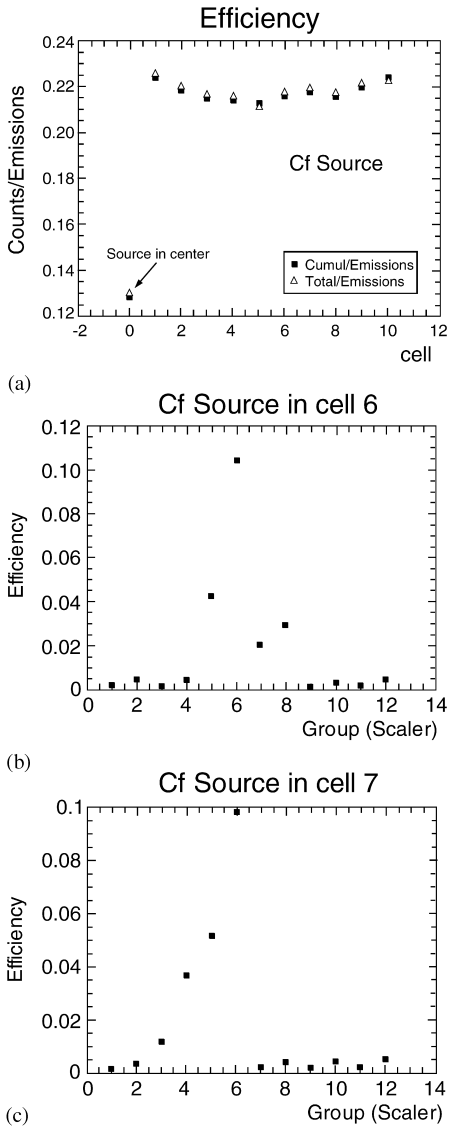

Fig. 7. The calibration efficiency. Statistical errors on the efficiency is 1%. See text for explanation of the symbols.

noted that, with the source both in cells 6 and 7, the closest subdetector is always the number 6 (see Fig. 1). The position of the peak in the distribution of counts does not change consequently. The distribution itself, however, varies because the relative position of the other subdetectors changes with respect to the source. The mean efficiency of the subdetector closer to the source was 10%.

5. Neutron emission results in cold fusion experiments

The detector was used in several Fleishmann–Pons like experiments [2–4]. While excess heat, ^{4}He and (moderate) Tritium production were detected, no neutron emission was observed. The few neutron candidates after the poissonian analysis did not pass the severe checks described in the previous paragraphs (pulse shapes, pulse charge distributions, position of the source by rotating the detector around its axes, etc.).

As an example, Fig. 8 shows the number of neutrons detected at 10 min intervals by subdetectors 1, 3, 6, 11, and 12 before and during the experiment. No statistical differences appear in the number of neutrons detected when electrolysis was in progress with the exception of two large counts in subdetector 12, which occurred at approximately 900 and 1200 h after the start of the experiment. However, the fact that the closest subdetectors (the eleventh above all) did not show any corresponding count enhancements proved that the counts of subdetector 12 were not generated by neutron emissions. The sources of these two enhancements of the subdetector 12 counts, as shown by a check at the oscilloscope, were anomalous pulses, in which a sudden very large negative drop of the signals were followed by oscillations around zero.

Count enhancements caused by electronic misfunctioning and lasting long-time intervals were also easily discovered. Efficient tools for this purpose were the pulse checking and the availability to

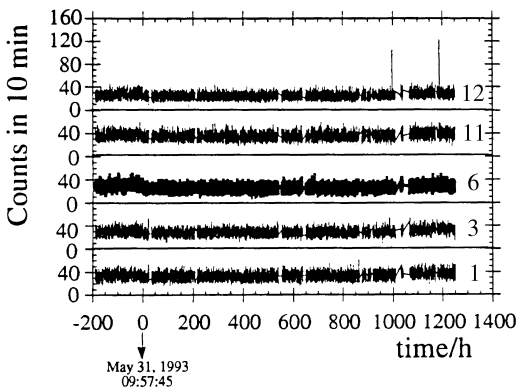

Fig. 8. Neutrons detection rates.

rotate the detector around its axis changing in this way the relative position of the subdetectors with respect to the hypothetical source.

The minimum neutron source detectable by our apparatus depended on the background rate and/or on the nature of the source itself. A time constant poisson-like source would have been detectable only if its average neutron emission substantially had increased one or more subdetectors counting rate. Our typical background, as shown in Fig. 8, had a subdetector rate of $m_b \sim 4$ counts/min. In the worst case of pure poissonian neutron source and with the detector efficiency quoted before, the minimum detectable source would have emit 60 neutrons/min according to our above-mentioned criterion (see Section 3). The level of rejection is much more conservative for potential cold fusion phenomena generating correlated neutrons.

Owing to the JSR the presence of emission of even such low sources just lasting some μs (and hence not detectable by the Pattern Unit used as coincidence unit) can be excluded.

6. Conclusions

A toroidal shape, large angular acceptance, segmented and rotating around its axis neutron detector was designed by INFN-Sanità group in order to cut out the cumbersome problems that usually grow up in cold fusion experiment. As a matter of fact, the toroidal shape of the detector allows both large angular acceptance and high efficiency and allocates room for several neutron sources to be placed inside it.

The segmentation of the detector allows the rough localization of a neutron source and improves the capability of background subtraction. Both digital and analog signals were provided by the detector. The former group is used for counting rates, the acquisition of the latter helps to cross out spurious pulses caused by electromagnetic noise.

The acquisition system is able to detect the number of neutrons even in case they are produced in very narrow burst. It is also able to check the presence of correlated source neutron emissions both when the neutrons are produced in very short burst or in long time intervals.

No significant neutron emissions (above 60 neutrons/min in the most conservative hypothesis of uncorrelated emissions) were detected in Fleishmann–Pons like experiments after the checks allowed by the geometry and the data acquisition system of the detector were performed.

References

[1] JSR-12, Neutron Coincidence Analyzer, Operation Manual, Canberra Industries, Inc., Jomar System Division, Los Alamos, December 1990.

[2] D. Gozzi, P.L. Cignini, R. Caputo, M. Tomellini, G. Balducci, G. Gigli, E. Cisbani, S. Frullani, F. Garibaldi, M. Iodice, G.M. Urciuoli, Experiments with global detection of cold fusion byproducts, in: H. Ikegami (Ed.), ICCF3, Proceedings of the Third International Conference on Cold Fusion, Nagoya, 21–25 October 1992, Frontiers of Science Series, Vol. 4, Universal Academy Press, Tokyo, 1993, p. 155.

[3] D. Gozzi, R. Caputo, P. Luigi Cignini, M. Tomellini, G. Gigli, G. Balducci, E. Cisbani, S. Frullani, F. Garibaldi, M. Iodice, G. Maria Urciuoli, J. Electroanal. Chem. 380 (1995) 91–107.

[4] D. Gozzi, F. Cellucci, P.L. Cignini, G. Gigli, M. Tomellini, E. Cisbani, S. Frullani, G.M. Urciuoli, J. Electroanal. Chem. 435 (1997) 113–136, [erratum J. Electroanal. Chem. 452 (1998) 251–271].